

Evolution of glacier-dammed lakes through space and time; Brady Glacier, Alaska, USA

Denny M. Capps*, John J. Clague

Centre for Natural Hazard Research, Department of Earth Sciences, Simon Fraser University, Burnaby, British Columbia V5A 1S6, Canada



ARTICLE INFO

Article history:

Received 13 November 2012
Received in revised form 7 December 2013
Accepted 9 December 2013
Available online 22 December 2013

Keywords:

Tidewater glacier
Glacier-dammed lake
Remote sensing
Brady Glacier
Glacier fluctuation

ABSTRACT

Glacier-dammed lakes and their associated jökulhlaups cause severe flooding in downstream areas and substantially influence glacier dynamics. Brady Glacier in southeast Alaska is well suited for a study of these phenomena because it presently dams 10 large ($>1 \text{ km}^2$) lakes. Our objectives are to demonstrate how Brady Glacier and its lakes have co-evolved in the past and to apply this knowledge to predict how the glacier and its lakes will likely evolve in the future. To accomplish these objectives, we georeferenced a variety of maps, airphotos, and optical satellite imagery to characterize the evolution of the glacier and lakes. We also collected bathymetry data and created bathymetric maps of select lakes. Despite small advances and retreats, the main terminus of Brady Glacier has changed little since 1880. However, it downwasted at rates of 2–3 m/y between 1948 and 2000, more than the regional average. The most dramatic retreat (2 km) and downwasting (120 m) have occurred adjacent to glacier-dammed lakes and are primarily the result of calving. Brady Glacier is a former tidewater glacier. With continued downwasting, Brady Glacier may return to a tidewater regime and enter into a phase of catastrophic retreat. The situation at Brady Glacier is not unique, and the lessons learned here can be applied elsewhere to identify future glacier-dammed lakes, jökulhlaups, and glacier instability.

© 2014 Elsevier B.V. All rights reserved.

1. Introduction

Glacier-dammed lakes and the catastrophic outburst floods (jökulhlaups) that emanate from them cause severe flooding in downstream areas and substantially influence glacier dynamics. Jökulhlaups commonly have peak discharge orders of magnitude larger than precipitation-induced floods (Clague and Evans, 1994). Large jökulhlaups can fracture and uplift glacier termini. The fracturing enhances mechanical removal of ice fragments, which can lead to the creation of large supraglacial channels and embayments (Russell et al., 2006). Jökulhlaups cause substantial erosion and deposition, alter riparian ecosystems (Post and Mayo, 1971), and have caused severe damage to infrastructure up to 1200 km from their source (Mason et al., 1930). Consequently, they are the farthest reaching of all terrestrial glacial hazards.

In the past decade, research has confirmed that glacier-dammed lakes and jökulhlaups can directly affect glacier motion. Jökulhlaups from Hidden Creek Lake in the Wrangell Mountains in Alaska increased horizontal glacier velocity up to six times (Anderson et al., 2005; Bartholomaeus et al., 2011). Sugiyama et al. (2007) recorded a temporary, but complete, reversal of horizontal glacier motion during a jökulhlaup in the Swiss Alps. Magnússon et al. (2010) noted an Icelandic glacier that accelerated after a jökulhlaup and did not return to its pre-flood state until several years later. Mayer et al. (2008) and

Walder et al. (2006) documented jökulhlaups from glacier-dammed lakes that were preceded by flotation, then deflation of the ice dams; flotation, in turn, caused a substantial intensification in calving and a manyfold increase in horizontal glacier velocity. Mayer et al. (2008) noted that the glacier experienced higher horizontal velocities into the former lake basin for two months after the jökulhlaup.

Brady Glacier, the largest glacier in the Fairweather Range of the St. Elias Mountains in Alaska, is well suited for a study of the evolution of glacial lakes. The main terminus of Brady Glacier has varied little over the past 130 years but, between 1948 and 2000, the lateral lobate margins of the glacier retreated up to 2 km and downwasted up to 120 m adjacent to 10 large ($>1 \text{ km}^2$) dammed lakes (Larsen et al., 2007; Capps et al., 2010). Six of the ten lakes are primarily subaerial (Fig. 1), and four are subglacial; we define a lake as subglacial if it occurs primarily underneath the glacier, whether or not it is at atmospheric pressure (Clague and Evans, 1994; Tweed and Russell, 1999). In seven of the ten lakes, the glacier has a calving margin that exceeds 1 km in width. These lakes, and many smaller ones, are in different stages of evolution—incipient, stable, and periodically draining.

Our goals in this paper are to demonstrate how Brady Glacier and the numerous lakes that it dams have co-evolved in the past and to apply this knowledge to forecast how the glacier and its lakes will likely evolve in the future. Our specific objectives are to (i) compile and interpret previous observations, research, maps, airphotos, and optical satellite imagery to define the last advance of Brady Glacier and the evolution of its lakes; (ii) describe the present state of the glacier and its lakes through the use of field-based measurements and recent

* Corresponding author at: Denali National Park and Preserve, P.O. Box 9, Denali Park, AK 99755, USA. Tel.: +1 907 683 9598; fax: +1 907 683 9639.

E-mail address: denny_capps@nps.gov (D.M. Capps).

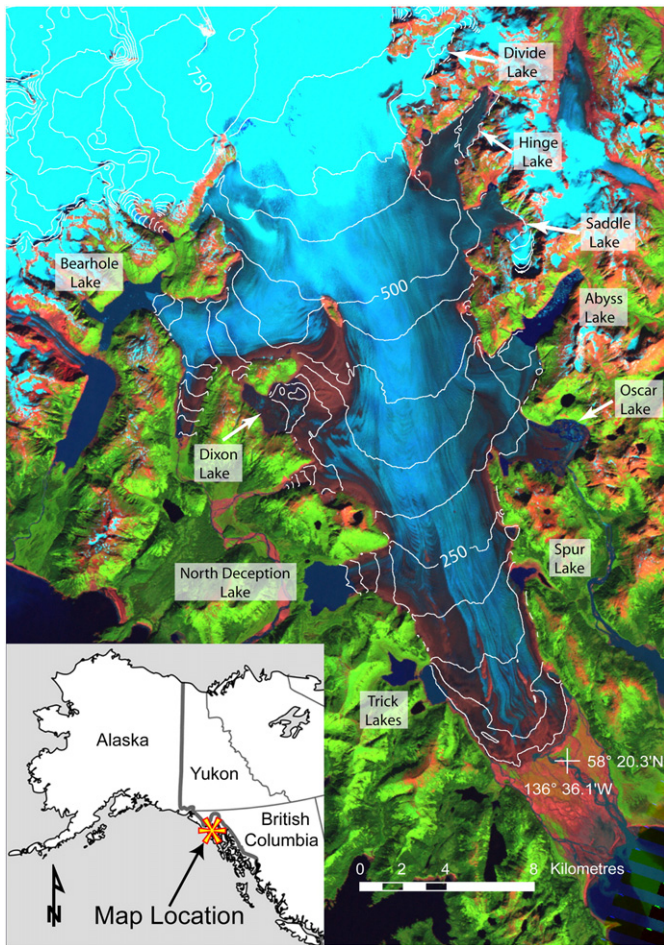


Fig. 1. False-colour Landsat 5 image (bands 7/4/2) of Brady Glacier, southeast Alaska, acquired on 14 August 2010. Topographic contours are derived from 2000 SRTM DEM (50-m contour interval).

optical satellite imagery; (iii) predict how the glacier and its lakes will evolve in the future based on analogous past behaviour in similar glacier systems in the region; and (iv) discuss how this information can be applied to forecast the future evolution of other glaciers and lakes in the region and elsewhere.

2. Regional setting

2.1. Brady Glacier

Brady Glacier is located in Glacier Bay National Park, 125 km west of Juneau, AK (Fig. 1). It is 51 km long and has an area of 590 km². In the early 1990s, the glacier had an accumulation area ratio (AAR) of 0.65, with an equilibrium line altitude (ELA) of ~610 m asl (Viens, 1995). Between 2003 and 2011, the glacier had an AAR of 0.40, with an ELA of ~745 m asl (Pelto et al., 2013). Peaks up to 3467 m asl to the north-west supply most of the ice to the glacier. The glacier terminates ~10 m asl on a large outwash plain that extends 4.8 km into Taylor Bay.

Brady Glacier lies within a NNW-trending, fault-controlled valley (Derksen, 1976) that is 65 km long and extends from Taylor Bay on the south to near the north end of Glacier Bay. An ice divide separates ice that flows SSE toward Taylor Bay as Brady Glacier and ice that flows NNW as Lamplugh and Reid glaciers to Glacier Bay (Bengtson, 1962; Derksen, 1976). The divide between south- and north-flowing ice lies at ~820 m asl based on the 2000 Shuttle Radar Topography Mission (SRTM) digital elevation model (DEM). Ice-penetrating radar measurements near the main axis of Brady Glacier indicate that the bed is

well below sea level and the valley might be a continuous fjord if the glaciers and outwash plain were not present (Barnes and Watts, 1977).

2.2. Previous studies

The late Holocene extent of Brady Glacier has been a subject of debate. The glacier had retreated at least 24 km north of its present terminus by 645–725 cal y BP, but began to advance shortly thereafter based on radiocarbon ages from subfossil wood in till (Bengtson, 1962; Derksen, 1976). Historical observations of the glacier date back to 1794 when Joseph Whidbey, Captain George Vancouver's lieutenant, made the first recorded observations of the terminus. The chart produced from his observations roughly reproduces the coastline (Vancouver, 1798), but the perspective is distorted. Numerous other explorers mapped the terminus area, but the changing glacier and inconsistent identification of landforms and reference points complicate interpretation of these early observations. Accurate maps of the area were not produced until detailed surveys were made in 1907.

Capps et al. (2011) determined the timing of the glacier's last advance and the related formation and filling of North Trick and Spur lakes, which formerly were probably marine embayments (Fig. 2). The lakes' inferred evolution is based on dendrochronology and precise, elevation-constrained mapping of overridden and drowned trees at the glacier margin. Brady Glacier impounded Spur Lake around 1830. Soon after 1839, Spur Lake reached an elevation of 125 m asl and began to overflow across a stable bedrock sill to the southeast. At a site 500 m northeast of North Trick Lake, the glacier thickened by at least 77 m between ca. 1844 and 1859. North Trick Lake was impounded by 1861 and rose to its highest elevation (ca. 130 m asl) when Brady Glacier reached its maximum extent around 1880. The glacier had begun to downwaste by 1929 when vegetation was once again growing in the area between the present lakeshore and the ca. 1880 strandline of North Trick Lake.

Several early explorers noted Brady Glacier's change from a tidewater glacier to one terminating on an outwash plain. George Vancouver, in his account of the 1794 exploration, wrote that '...further progress was now stopped by an immense body of compact perpendicular ice, extending

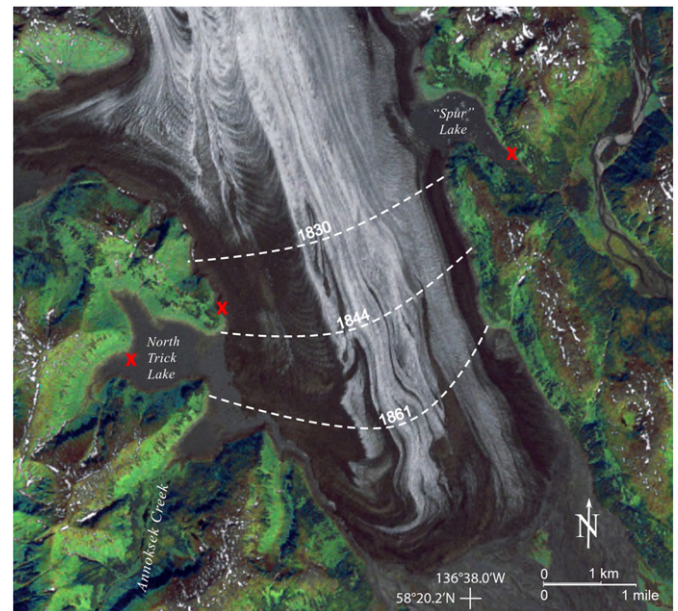


Fig. 2. Inferred terminus of Brady Glacier at three times during the nineteenth century, based on death dates of trees that were killed by overriding glacier ice or drowned in lakes dammed by the advancing glacier (from Capps et al., 2011). Red 'x's indicate sampling areas. Landsat 7 ETM + mosaic (bands 3/2/1) acquired 1999–2002.

from shore to shore' (Vancouver, 1798, p. 242), which indicates a tide-water terminus. By 1880, however, John Muir commented, 'No icebergs are discharged from it, as it is separated from the water of the fiord at high tide by a low, smooth mass of outspread, overswept moraine material... The front of the glacier, like all those which do not discharge icebergs, is rounded like a brow, smooth-looking in general views...' (Muir, 1915, p. 295–296). Therefore, sometime between 1794 and 1880 the terminus evolved from a calving margin into a noncalving margin.

3. Methods

3.1. Evolution of Brady Glacier through time

We georeferenced a variety of maps, airphotos, and optical satellite imagery (Table 1) to delineate Brady Glacier from the beginning of the twentieth century to 2010. As previously noted, the earliest map of the area is from 1794, but the first topographic map with ice contours was made in 1907 during the Canada–U.S. International Boundary Survey (International Boundary Commission, 1923). We scanned the latter map at a resolution of 600 dots per inch (dpi). The first airphotos of the area were taken in 1929 by the United States Navy, but these only cover the lowest 10 km of the glacier. The first large-scale, high-quality maps of the entire glacier were produced from airphotos taken in 1948. More airphotos were taken periodically through 1997. Glacier Bay National Park provided us with 600 dpi scans of the 1929 airphotos and 1997 digitally-orthorectified black-and-white airphotos. The 1997 airphotos were the foundation for our GIS work because of their high spatial resolution (1 m). We obtained 600 dpi digital scans of the 1948 and 1979 airphotos and Landsat imagery from the U.S. Geological Survey's EarthExplorer web server (<http://edcns17.cr.usgs.gov/EarthExplorer/>). The earliest satellite imagery used here is from Landsat 1, acquired in 1972. Repeat Landsat 5 and 7 imagery is available to the termination of our study in 2010.

Using the georeferencing tool in ArcGIS 9.3 and techniques outlined in Hughes et al. (2006), we identified at least eight ground control points (GCPs) per airphoto or map, applied a second-order polynomial transformation, and resampled pixels through cubic convolution. From these georeferenced products, we manually outlined the glacier terminus for the years 1907 and 1929, and the glacier below the ELA for the years 1948, 1979, 1997, and 2010.

Table 1
Imagery utilized in this study.

Date	Source	Scale/resolution	Bands
1907	IBC maps	1:250,000 scale	N/A
1929	Navy airphotos	1:20,000 scale	N/A
1948	B/W airphotos	1:40,000 scale	N/A
1948	USGS topographic maps	1:63,360 scale	N/A
1948	NED DEM	45 m resolution	N/A
8/11/1972	Landsat 1	60 m resolution	7/5/4
7/25/1977	Landsat 2	30 m resolution	7/5/4
1979	CIR airphotos	1:63,360 scale	N/A
10/3/1981	Landsat 2	30 m resolution	7/5/4
8/21/1986	Landsat 5 TM	30 m resolution	7/4/2
9/6/1986	Landsat 5 TM	30 m resolution	7/4/2
8/19/1990	Landsat 5 TM	30 m resolution	7/4/2
4/24/1995	Landsat 5 TM	30 m resolution	7/4/2
1997	DOQ airphotos	1 m resolution	N/A
8/1/1999	Landat 7 ETM +	30 m resolution	7/4/2
2/2000	SRTM DEM	30 and 90 m resolution	N/A
1999–2002	Landat 7 ETM + mosaic	30 m resolution	3/2/1
8/3/2009	Landsat 5 TM	30 m resolution	7/4/2
8/14/2010	Landsat 5 TM	30 m resolution	7/4/2
8/15/2010	Landat 7 ETM +	30 m resolution	7/4/2
9/16/2010	Landat 7 ETM +	30 m resolution	7/4/2
9/19/2010	Landsat 5 TM	30 m resolution	7/4/2

We determined the volume change of the glacier through time using elevation change data supplied by Dr. Chris Larsen of the University of Alaska Fairbanks. Larsen et al. (2007) differenced the 2000 SRTM DEM from the National Elevation Dataset DEM, which is based on the airphotos taken in 1948, to determine elevation and volume changes of Brady Glacier and other glaciated areas of southeast Alaska and adjacent British Columbia, Canada. They published a regional map of glacier elevation changes that includes Brady Glacier; however, the scale is too small for the detail needed in this study. They also plotted volume change rates of Brady Glacier in comparison to other glaciers in the region, but did not provide numerical values. Regardless, we wanted to calculate separate values of volume change in the ablation and accumulation zones. Therefore, using a GIS, we created a map of elevation change based on all pixels over the glacier from Larsen's data (45-m spacing) and calculated from those values the glacier volume change between 1948 and 2000. We estimated the volume error by multiplying the DEM differencing error (± 0.3 m/y below the ELA and ± 0.6 m/y above the ELA) by the glacier area. The differencing error is greater in the accumulation zone because of the larger error associated there with photogrammetric mapping (Larsen et al., 2007).

3.2. Evolution of Brady Glacier lakes and jökulhlaups through time

We identified and characterized Brady Glacier lakes from the beginning of the twentieth century to 2010 with the same georeferenced GIS data that we used to delineate the glacier (Table 1). Quantified attributes include area, width of calving front, and elevation. We also compiled evidence of past jökulhlaups and drainage routes based on previous research, field observations, and optical imagery. Earlier jökulhlaups were recorded primarily by Post and Mayo (1971) and Derksen (1976). Since the mid-1970s, most evidence of jökulhlaups consists of observations of unusually turbid, debris- and iceberg-laden water adjacent to the glacier made by Glacier Bay National Park personnel or reported to the park by passing boat captains.

3.3. Current bathymetry of select glacier-dammed lakes

We collected bathymetry data and created bathymetric maps of Abyss, Bearhole, East Trick, North Deception, and Oscar lakes (Fig. 1) using a sonar-equipped floatplane and a custom-built, remote-controlled boat. The sonar was a consumer-grade, GPS-enabled, Lowrance LCX-17 M. We collected data on the dual frequency setting (50/200 kHz), which allowed for high definition in shallow water (<100 m) and greater penetration in deeper lakes (>100 m). We made spot checks to confirm that the sonar was accurate in the turbid glacier-dammed lakes using a manual measuring line. Data in larger stretches of open water at a relatively safe distance from the calving front of the glacier were collected from the floatplane. We used the remote-controlled boat to collect data near the more hazardous calving fronts. With one exception, we created bathymetry maps using the default settings of Golden Software Surfer 9 software and the minimum curvature gridding method. In the case of North Deception Lake, the default setting produced an unnatural cross shape in the bathymetry. To produce a more realistic interpretation, we changed the internal tension settings from 0 to 1.

4. Results

4.1. Evolution of Brady Glacier through time

Changes in the position of the front of Brady Glacier since the end of the Little Ice Age have been small compared to those of other glaciers in the region (Larsen et al., 2007; Barclay et al., 2009). The greatest change occurred between 1948 and 1979 when the glacier advanced by as much as 600 m (Fig. 3). However, for a 51-km-long glacier, this advance is relatively small (~1%). Between 1979 and 2010, the glacier front

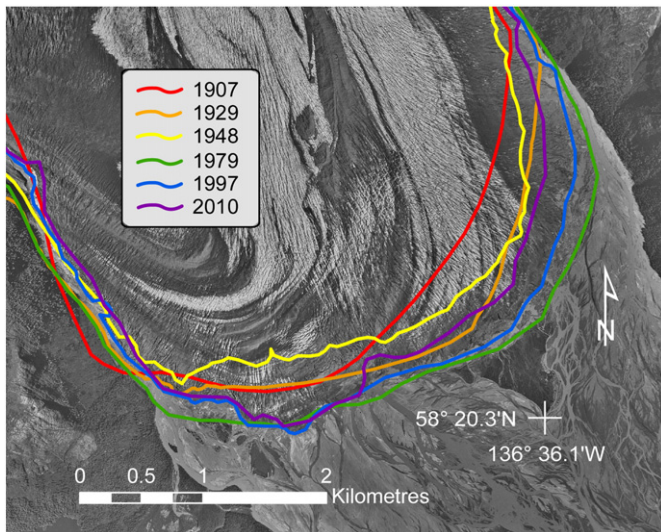


Fig. 3. Location of the Brady Glacier terminus through time based on georeferenced maps, airphotos, and Landsat imagery from 1907 to 2010. The background image is a 1997 digitally orthorectified quadrangle.

retreated up to 450 m. In the late 2000s and 2010, small lakes began to form at the terminus (Fig. 1).

Although the main front of Brady Glacier has moved little since 1907, the glacier has downwasted substantially, particularly in areas adjacent

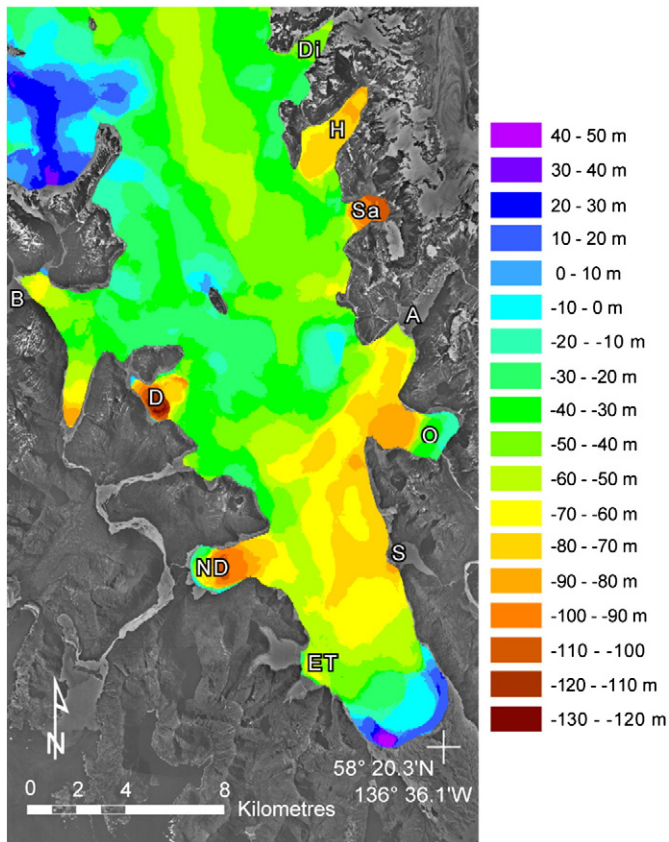


Fig. 4. Brady Glacier elevation change from 1948 to 2000. The background image is a 1997 digitally orthorectified quadrangle. Glacier-dammed lakes indicated by letters, clockwise from top right: Di—Divide Lake, H—Hinge Lake, Sa—Saddle Lake, A—Abyss Lake, O—Oscar Lake, S—Spur Lake, E—East Trick Lake, ND—North Deception Lake, D—Dixon Lake, B—Bearhole Lake.

to the glacier-dammed lakes (Fig. 4). Assuming an ELA of 610 m asl (Viens, 1995), glacier volume loss between 1948 and 2000 is $9.5 \pm 2.9 \text{ km}^3$ in the ablation zone and $4.5 \pm 8.1 \text{ km}^3$ in the accumulation zone, for a total volume loss of $14.0 \text{ km}^3 \pm 11.1 \text{ km}^3$. The greatest downwasting is adjacent to Dixon Lake ($\sim 125 \pm 16 \text{ m}$), Saddle Lake ($111 \pm 16 \text{ m}$), and North Deception Lake ($103 \pm 16 \text{ m}$). Despite the overall pattern of downwasting, some areas seem to have thickened. Fig. 4 shows 40–50 m of thickening at the southeast margin of the terminus. This result is supported by Fig. 3, which shows that the glacier advanced in this area from 1948 to 1979. Fig. 4 also shows as much as 30–40 m of thickening in the northwest part of the map, which is in the accumulation zone. We were unable to verify if this apparent thickening is real or an error associated with the difficulties of photogrammetric mapping in the low-contrast accumulation area of the glacier (Aðalgeirsdóttir et al., 1998; Arendt et al., 2002).

4.2. Evolution of Brady Glacier lakes and jökulhlaups through time

Direct comparisons of Brady Glacier lakes and jökulhlaups through time are difficult because they are dynamic features and events. An airphoto or satellite image only shows a lake's condition at a specific time and does not indicate whether the lake is filling, stable, or rapidly draining. To address this issue, the lakes and their associated jökulhlaups must be discussed individually in the larger context of their histories and settings. However, Table 2 summarizes lake elevation and calving width through time and whether or not jökulhlaups were occurring during this study.

4.2.1. Bearhole Lake

Bearhole Lake is first identifiable in airphotos taken in 1948, when it appears as three lobes of open water between Brady and Palma glaciers and tributary valleys (Fig. 5). At that time, the lake had a combined surface area of 0.8 km^2 , was dammed to an elevation of $\sim 205 \text{ m asl}$ by Palma and Brady glaciers, and had a combined calving front over 2300 m long (Table 2). Jökulhlaups drained subglacially under Palma Glacier into Palma River (Fig. 5). Dendrochronology indicates that catastrophic floods from this lake denuded the floodplain of Palma River around 1918, and floods continued to at least 1976 (Derksen, 1976). The lake continued to be dammed by Palma Glacier at least through 1979, but by 1997 Palma Glacier had retreated and downwasted enough that Bearhole Lake was dammed at a lower elevation by a bedrock sill to the southwest and Brady Glacier to the southeast. We found no evidence that the lake has experienced further jökulhlaups since that time. In 2010, the lake had an area of 3.2 km^2 and the calving margin had retreated into a relatively stable position in a constriction in the Bearhole lobe of Brady Glacier (Fig. 1).

4.2.2. Dixon Lake

Dixon Lake is first evident in the 1948 airphotos as a 0.8-km^2 iceberg-choked subaerial lake. The lake drained subglacially to the south and west before emerging subaerially into Dixon River (Fig. 5). Photographs taken from adjacent peaks in 1894 by the International Boundary Commission show the valley floor of Dixon River stripped of vegetation and full of sediment, that the lake was likely dammed and releasing jökulhlaups at that time. It was either subglacial or not properly surveyed on the 1907 topographic map. Dixon Lake underwent major change in the 1980s when a large area of glacier ice around its margin began to float. By the 1990s, the floating margin was beginning to break up; and then, during the 2000s, subaerial Dixon Lake grew rapidly in size. In 2007, one of us (DMC) witnessed the draining of the lake, the subglacial discharge of floodwaters from Dixon Lake, inundation of the floodplain of Dixon River, and large standing waves and a sediment plume where the river enters Dixon Harbor. By 2010, Dixon Lake had grown to 3.6 km^2 and was the largest lake dammed by Brady Glacier.

Table 2
Attributes of lakes dammed by Brady Glacier^a.

Lake	m a.s.l.		~Calving margin width (m)		Interpolated minimum volume of select lakes (m ³)	Present jökulhlaups?
	1948	2000	1948	2010		
Bearhole	204	165	2360	1850	1.3 × 10 ⁸	No
Dixon	274	170	940	2820		Yes
North Deception	23	18	2150	1270	9.5 × 10 ⁷	No
North Trick	60	30	760	nc		No
East Trick	nl	30	nc	1660	1.5 × 10 ⁷	Rarely
South Trick	60	30	920	nc		No
Spur	133	133	1190	1140	6.5 × 10 ⁷	Yes
Oscar	198	198	770	6400		No
Abyss	269	230	890	1240	3.45 × 10 ⁸	Yes
Saddle	507 ^b	411 ^b	900	1300		Possibly ^c
Hinge	501 ^b	430 ^b	610	610	Possibly ^c	
Divide	624 ^b	584 ^b	nc	nc	Possibly ^c	

^a Notes: nl—lake did not exist at that time.

^b Elevation of ice shelf; nc—no calving margin.

^c See Capps et al., 2010.

4.2.3. North Deception Lake

This lake was first dammed between the west-flowing North Deception lobe and a NNE-trending ridge, as shown on the 1907 topographic map (Fig. 6A). We found no documented evidence for jökulhlaups from this lake, but any such floods would have drained into adjacent Dixon River (Fig. 5). When full, the lake may have backed up into South Deception Lake. By 1929, the glacier had begun to retreat and North Deception Lake occupied an overdeepened depression produced by the North Deception lobe. The lake entered a phase of relative stability for several decades, but beginning in the mid-1990s, the North Deception lobe began to break up rapidly and retreat to the east. By 2004, the ice margin had retreated to a more stable position where the lobe narrows, and it has remained near that position since. The surface area of the lake

increased from 0.5 km² in 1948 to 3.2 km² in 2010. Comparison of contours in Fig. 6B and glacier recession in Fig. 6C indicates that over 150 m of glacier thinning has occurred at North Deception Lake between 1948 and 2010, consistent with the findings of Larsen et al. (2007). The surface of the lake has lowered only slightly since 1948 because a stable lower outlet was established during glacier retreat. We found no evidence that North Deception Lake has produced jökulhlaups.

4.2.4. North Trick Lake

Dendrochronologic evidence indicates that North Trick Lake formed by 1861 when the glacier was advancing (Capps et al., 2011). The lake is shown on the 1907 topographic map but is not accurately delineated (Fig. 7A). By 1929, the glacier was downwasting, the lake was dammed at a lower level, and vegetation was colonizing the area between the lakeshore and the highest strandline (Fig. 7B). The 1948 airphotos show the lake at an even lower level, with at least three, progressively less densely vegetated strandlines above the shoreline (Fig. 7C). Post and Mayo (1971) and Derksen (1976) noted that North Trick Lake has a long history of jökulhlaups. The lowest nonglacial outlet of the basin is at ~245 m asl, or ~115 m higher than the highest strandline. Because the lake does not have a stable outlet, it would fill and drain repeatedly, presumably beginning not long after it formed and filling the basin to near nine-tenths the height of the glacier dam. North Trick Lake drained to South Trick Lake (Fig. 5). By the mid-1980s, Brady Glacier had retreated sufficiently that it no longer dammed North Trick Lake (Fig. 7D). Today, the lake is a stable 1.0-km² moraine-dammed lake.

4.2.5. South Trick Lake

This lake likely formed a few years after North Trick Lake, but before the glacier reached its maximum extent in ca. 1880 (Bengtson, 1962; Derksen, 1976; Capps et al., 2011). It is shown on the 1907 topographic map, but like North Trick Lake, its basin is not accurately delineated (Fig. 7A). In the 1929 airphotos, the lake has an area of 0.7 km² and is full and overflowing into Annoksek Creek (Fig. 5). In the 1948 airphotos, it is lower and is not discharging into Annoksek Creek. At that time, however, it still had an area of 0.7 km² because the glacier front had retreated. By the mid-1980s, the glacier had retreated farther and no longer dammed South Trick or North Trick lakes; the two lakes began to merge into one larger lake that we call East Trick Lake. Based on changes in vegetation evident in Landsat imagery between 1986 and 1990, East Trick Lake no longer reached an elevation that allowed it to overflow into Annoksek Creek; instead it drained catastrophically onto Brady Glacier's outwash plain. Beginning in the early 2000s, East Trick Lake was no longer dammed to sufficient elevations to be confluent with South Trick Lake. South Trick Lake was left as an isolated 0.2-km² moraine-dammed lake. As late as 2009, East Trick Lake occasionally reached a level at which it became confluent with North Trick Lake.

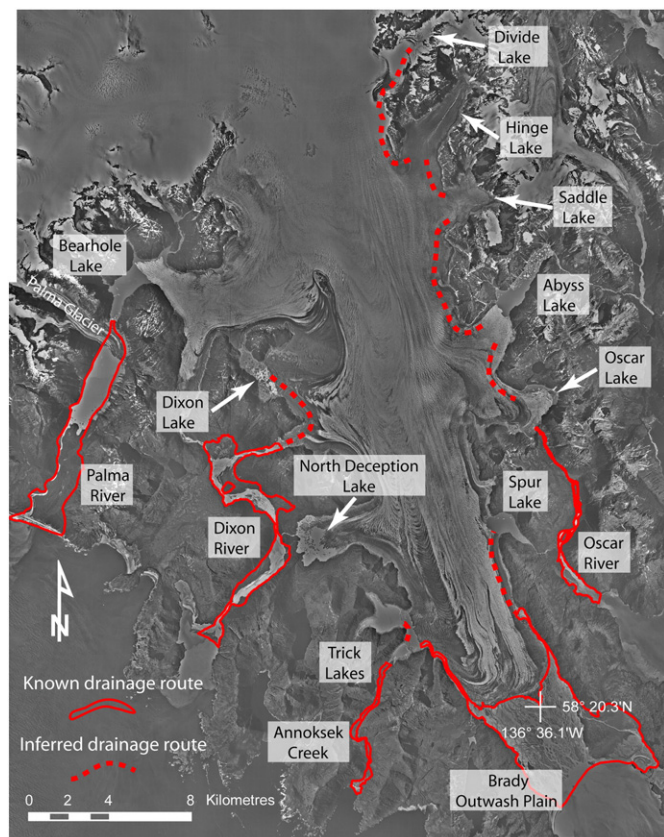


Fig. 5. Map of large glacier-dammed lakes (>1 km²) and historic jökulhlaup drainage routes. The background image is a 1997 digitized orthorectified quadrangle.

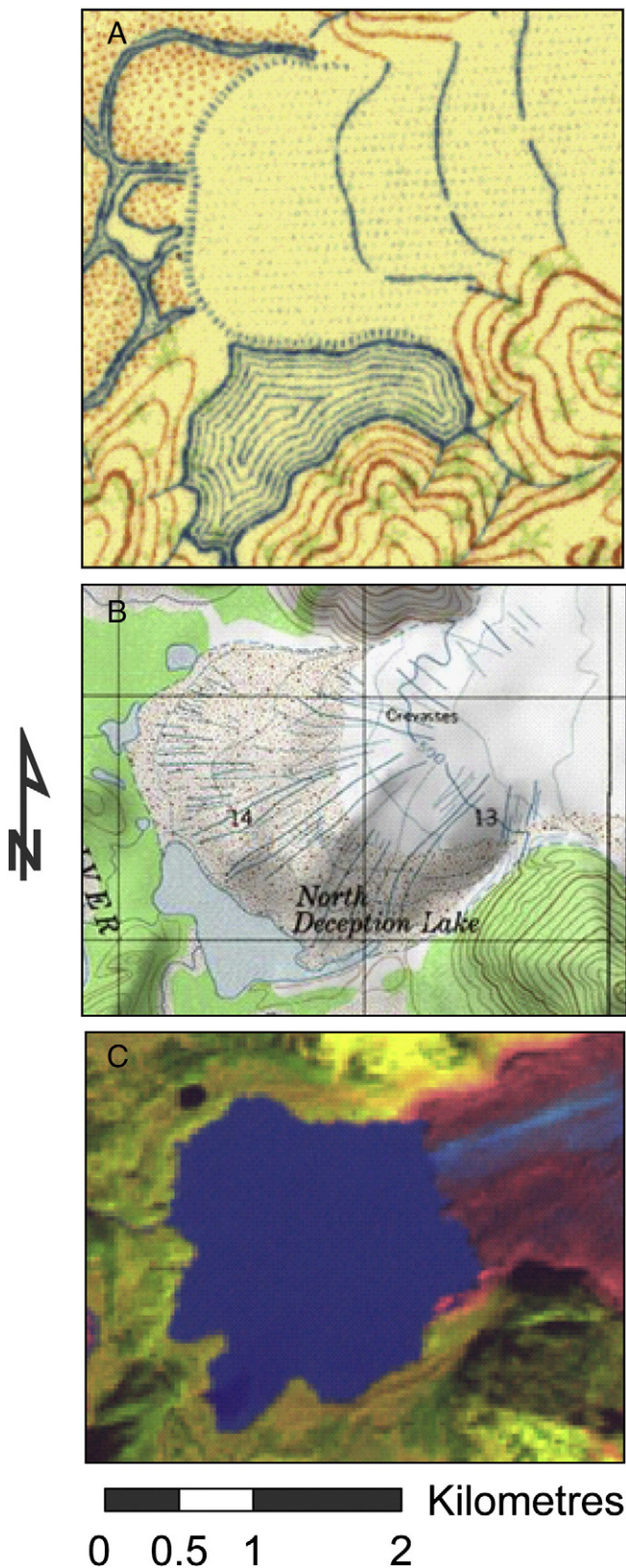


Fig. 6. Evolution of North Deception Lake. (A) 1907 International Boundary Commission 1:250,000-scale topographic map; contour interval 250 ft (ca. 75 m). (B) 1948 U.S. Geological Survey 1:63,360-scale topographic map; contour interval 100 ft (ca. 30 m). (C) 15-m resolution, false-colour Landsat 7 ETM + image (bands 7/4/2), acquired on September 16, 2010.

4.2.6. Spur Lake

Spur Lake began to form before 1830 and had filled to near its stable outlet at ~125 m asl by ca. 1839 (Capps et al., 2011). It had an area of 0.4 km² in 1929. By 1948 the lake had increased in area to 0.8 km² through retreat of the calving glacier margin while maintaining the same elevation. Spur Lake does not appear to have produced a jökulhlaup until recently. The lake apparently remained full prior to a Landsat image acquired in March 2002, which showed it in a partially drained state. Since then, jökulhlaups have partially drained the lake to the terminus of the glacier (Fig. 5), the lake has not filled to its upper stable outlet, and vegetation is becoming established below the highest strandline. Stranded icebergs observed in the basin in 2007 by DMC indicate that jökulhlaups have continued. When at lower levels, a portion of Spur Lake is dammed by a lateral moraine (Fig. 1). The area of the lake on 16 September 2010, was 0.6 km².

4.2.7. Oscar Lake

This lake appears as a small (0.1-km²) subaerial lake on the 1907 topographic map and is about the same size on the 1948 topographic map. The lake probably had a much larger subglacial area in 1948 based on the relatively flat surface of the adjacent ice lobe; the very low surface slope of the ice is characteristic of a floating margin. Since 2000, the width of the calving front and the subaerial area of the lake have increased rapidly from thinning and breakup of ice, which are evident in Landsat imagery. By 2010, the surface area of the lake had increased to 2.6 km². The level of the lake, however, has remained constant because it is controlled by a bedrock sill at ~200 m asl. Oscar Lake has no known history of jökulhlaups.

4.2.8. Abyss Lake

The area that is now Abyss Lake appears as flat or nearly flat ice on the 1907 topographic map. The 1948 map shows a 2.6-km² subaerial lake dammed by Brady Glacier on the southwest and overflowing across a bedrock sill to the east at ~270 m asl. The lake has partially emptied most years since 1994, draining subglacially into Oscar Lake and over a bedrock sill into the Oscar Creek drainage (Fig. 5), where the floodwaters have caused widespread damage to forest. The 1994 jökulhlaup, which caused the level of Abyss Lake to fall 77 m, released ~130 × 10⁶ m³ of water and was the first known flood in the Oscar Creek catchment for at least 80 years based on dendrochronological evidence (Glover, 2003). The elevation of the lake was ~40 m lower in 2000 (SRTM DEM data) than in 1948 (topographic map), although the former level was measured in February 2000, a time of year when the lake is commonly lower after a summer outburst. Nonetheless, observations during three seasons of fieldwork (2005–2007) and satellite imagery indicate that the lake may no longer fill to the level of the bedrock sill on the east. The width of the calving front in Abyss Lake increased almost 40% from 1948 to 2010. The surface area was 2.7 km² in 2010, an increase of only 4% from 1948. Although almost 0.4 km² of ice has been lost in the Abyss embayment, the westward expansion of the lake has been offset by the fall in lake level and the consequent smaller surface area around its perimeter. Abyss Lake probably extends far underneath Brady Glacier based on the extensive, flat ice shelf at the margin of the lake.

4.2.9. Subglacial lakes

Capps et al. (2010) identified three subglacial lakes north of Abyss Lake, which they informally named Saddle, Hinge, and Divide lakes. Only small areas of water are exposed seasonally along the margins of each of these lakes. Saddle Lake is ~2.0 km long and 1.6 km wide and has a saddle-shaped perimeter. The lake underlies a distributary lobe that flows eastward before spilling into embayments to the northeast and southeast. A part of the lake in the southeast embayment underlies the distributary lobe and a small tributary glacier flowing to the north. The suture zone between the two glaciers is evidenced by an accumulation of surface debris (Fig. 1). Hinge Lake is ~4.2 km long, 1.3 km wide, and has a distinctive hinge-like crevasse that runs along the axis of a

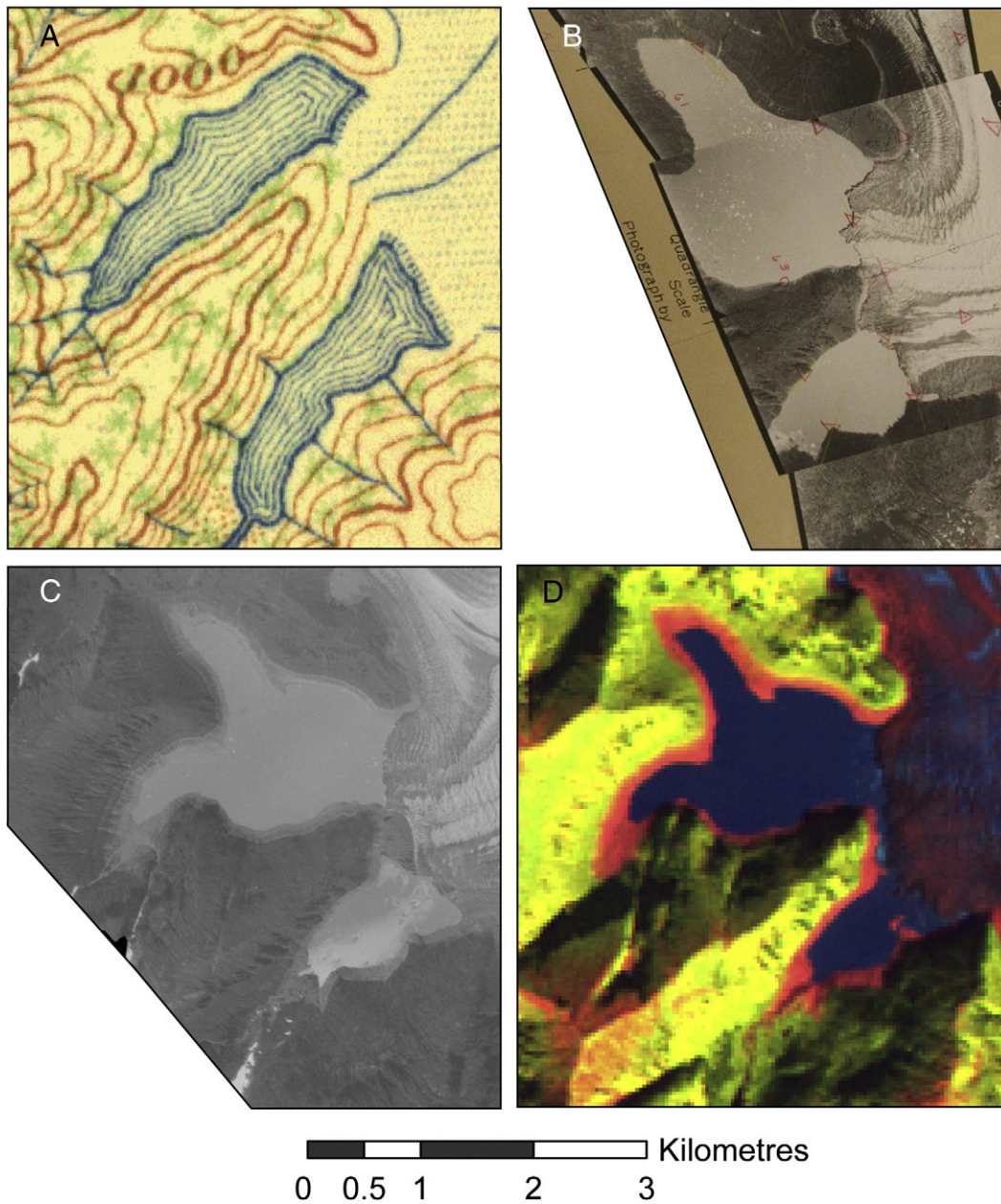


Fig. 7. Evolution of the Trick lakes. (A) 1907 International Boundary Commission 1:250,000-scale topographic map; contour interval 250 ft (ca. 75 m). (B) 1929 U.S. Navy 1:20,000 scale airphoto. (C) 1948 U.S. Geological Survey 1:40,000 scale airphoto. (D) 30-m resolution, false-colour Landsat 5 image (bands 7/4/2) acquired on September 6, 1986.

northeast-trending distributary lobe. The crevasse is likely the result of repeated filling and draining of the lake. Divide Lake is ~1.5 km long and 0.5 km wide. It is near the Brady Glacier ice divide below Divide Peak and underlies a northeast-trending distributary glacier. None of the three lakes has a known history of jökulhlaups. However, analysis of InSAR data has shown that from September 1995 to March 1996 Saddle Lake discharged over 300,000 m³ of water, Hinge Lake over 600,000 m³, and Divide Lake over 50,000 m³ (Capps et al., 2010).

4.3. Bathymetry of select glacier-dammed lakes

We collected sonar depth data and created bathymetric maps of Abyss, North Deception, East Trick, Bearhole, and Oscar lakes (Fig. 8). The bathymetry map of Abyss Lake (Fig. 8A) represents water depths when the lake is full, even though it was partially drained when we conducted the survey. Because of the challenges of collecting

bathymetry data in many glacier-dammed lakes, the density of survey lines is low and interpolation between lines likely underestimates actual lake volumes (Table 2). For example, the northwest and northeast arms of Bearhole Lake are shown in Fig. 8D as being ≤25 m deep. However, no bathymetry data were collected in those parts of the lake because of high iceberg concentrations, and the interpolation procedure probably underestimates water depths and thus volumes. In general, the lake volumes presented in Table 2 should be considered minimum estimates.

5. The effect of calving on Brady Glacier

The greatest retreat (2 km) and downwasting (~125 m) of Brady Glacier have occurred adjacent to glacier-dammed lakes. In the discussion that follows, we examine the ways in which glacier-dammed lakes can affect glacier retreat and downwasting.

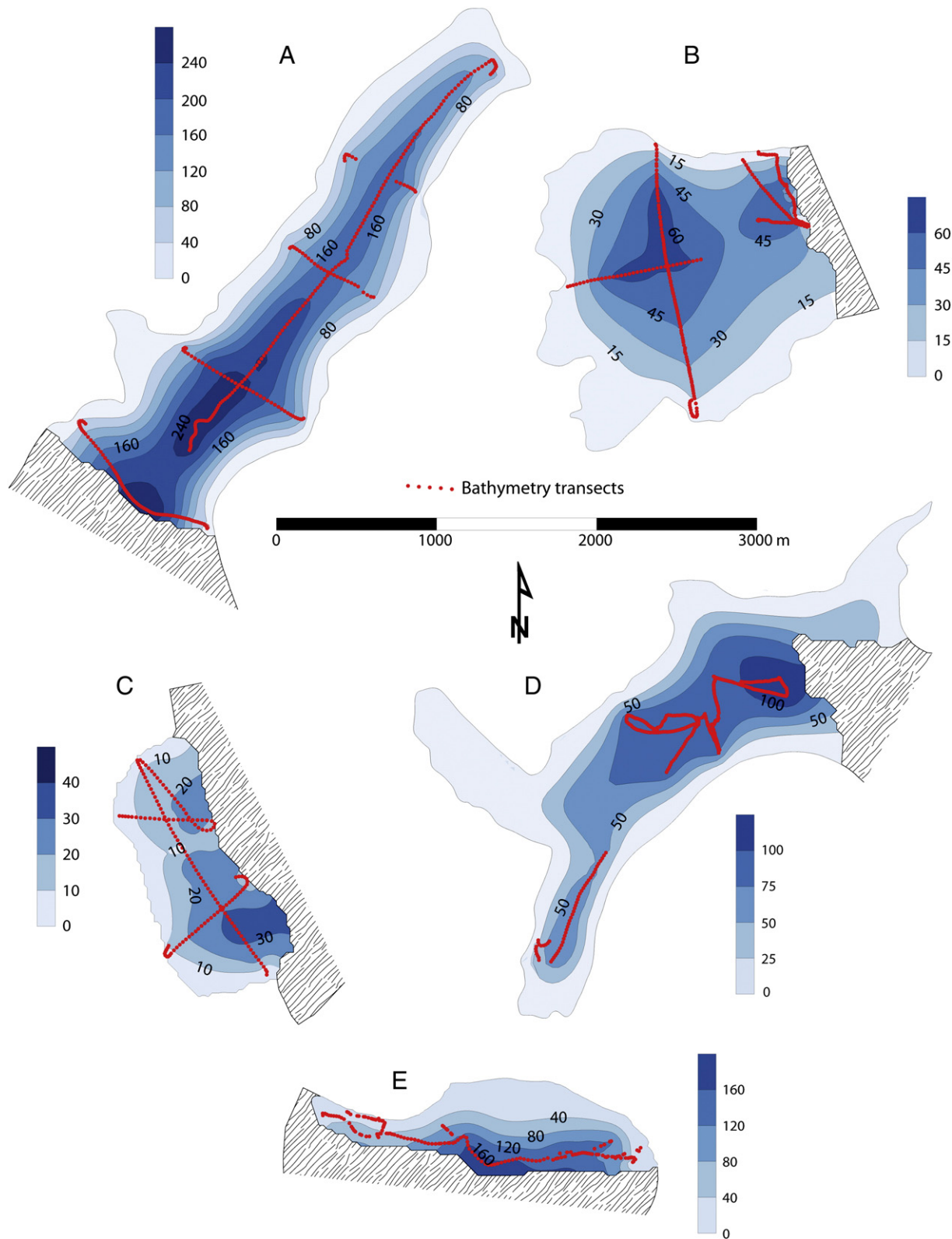


Fig. 8. Bathymetric maps of selected Brady Glacier lakes. Patterned area is glacier. (A) Abyss Lake when full to overflow, (B) North Deception Lake when full to overflow, (C) East Trick Lake on 29 August 2005, (D) Bearhole Lake when full to overflow, and (E) Oscar Lake on when full to overflow.

5.1. Terminal calving

Tidewater glaciers are more strongly influenced by the nature of the terminus than other glaciers. For example, adjacent Glacier Bay is the site of the greatest documented glacier retreat in history; the tidewater

glacier there retreated over 100 km in 145 years until it stabilized in shallow water (Vancouver, 1798; Molnia, 2008). While Brady Glacier is not currently a tidewater glacier, it was in the late 1700s and may return to that regime. It is different from most other glaciers in the region in that its terminus has changed little over the past 13 decades in spite

of extensive downwasting. If the glacier continues to downwaste, which is likely in the prevailing climate, its terminus must eventually retreat (Pelto et al., 2013). Brady Glacier is grounded well below sea level (Barnes and Watts, 1977), which keeps the terminus in an extended position even though it is actively downwasting. Assuming that other variables do not change, downwasting causes a decrease in effective pressure at the bed. A decrease in effective pressure can cause a glacier to flow faster (Meier and Post, 1987). Alternatively, Brady Glacier may have maintained a constant velocity with a reduced surface slope while maintaining an extended terminus.

Brady Glacier is beginning to retreat in sensitive areas, evidenced by small lakes that are beginning to form around the perimeter of the main terminus. If these small lakes grow in size, they may eventually coalesce with enlarging East Trick Lake 3 km to the north and become large enough to return the main terminus of the glacier to a lake-calving regime. The removal of back-pressure because of calving at the ice front can also cause an increase in velocity, which may initiate a positive feedback cycle (Meier and Post, 1987). If Brady Glacier were to return to a calving regime, it would retreat until the terminus stabilized in shallower water. As Brady Glacier begins to retreat, its outwash plain will act as a stabilizer by confining icebergs in a small area, which will slow the calving process by buttressing the ice margin (van der Veen, 2002; Geirsdóttir et al., 2008). Through time, however, this effect will diminish as the terminal lake grows larger and the outwash plain possibly is eroded (see Section 5.3).

5.2. Glacier-dammed lake margins

Margins of glacier-dammed lakes, like those of tidewater glaciers, are major foci of ice loss. The areas of Brady Glacier that have experienced the greatest downwasting and retreat over the past 130 years are adjacent to glacier-dammed lakes. If other factors are constant, an increase in calving width will cause an increase in mass loss. In 1948

the large lakes described in this study had a combined calving width of 11.5 km; by 2010 the width had increased to 18.3 km, an increase of 63%. Additionally, as the calving margins retreated into deeper water, larger icebergs calved, which facilitated further mass loss. We know the bathymetry of several lakes from SONAR data (Fig. 8) and the generalized bathymetry of Dixon Lake from aerial observations when it was partially drained (Fig. 9). Increased calving width and iceberg thickness combined to contribute to the large downwasting and retreat at the lakes. Divide Lake experienced the least downwasting, probably because it is nearest the ELA and does not have a calving margin like the other lakes.

We know from field observations and satellite imagery (Fig. 1) that the glacier built substantial subaqueous moraines at the grounding lines of North Trick, South Trick, and Spur lakes where the margin was stable for an extended period. Once the glacier margin retreated from these moraines, ice loss increased because a reverse-slope bed allowed thicker blocks of ice to calve in the deeper water.

Glacier-dammed lakes can cause large amounts of ice-mass loss by calving associated with jökulhlaups. Many glacier-dammed lakes have a floating ice tongue that collapses when the lake begins to drain (Marcus, 1960; Walder et al., 2006; Mayer et al., 2008). Jökulhlaups at Tulsequah Lake and Lake No Lake, both of which are dammed by Tulsequah Glacier in northwestern British Columbia, generated so much calved ice that the water was obscured (Marcus, 1960; Geertsema and Clague, 2005). The senior author observed this phenomenon during the 2007 draining of Dixon Lake. In previous days, the lake had large areas that were iceberg-free. As the lake drained and the floating ice tongue was no longer supported, the lake became covered with icebergs (Fig. 9). After an ice tongue fragments in such a scenario, the ice melts faster and is more readily transported out of the lake during a jökulhlaup, thus removing mass more rapidly from the glacier. This process is repeated each time the lake drains and refills as long as a floating tongue reforms.



Fig. 9. Dixon Lake partially drained during a jökulhlaup in August 2007. The lake is ~2.3 km long.

5.3. Possible jökulhlaup effects on the stability of Brady Glacier

A large jökulhlaup or series of jökulhlaups could erode Brady Glacier's terminus and the adjacent outwash plain. Russell et al. (2006) noted that mechanical breakup of glacier ice is one of the most distinctive effects of jökulhlaups. Processes that could impact Brady Glacier include (i) large-scale tunnel collapse; (ii) hydraulic jacking along the glacier margin and surface; and (iii) undercutting of the margin, causing ice-cliff collapse. A catastrophic jökulhlaup from the combined Abyss–Oscar lake system poses the greatest present risk to the stability of the main terminus of Brady Glacier. We know from past jökulhlaups that Abyss Lake is hydraulically connected to Oscar Lake through a subglacial conduit or conduits. Even after Abyss Lake has drained into Oscar Lake, as it has in past years, it contains at least $2.1 \times 10^8 \text{ m}^3$ of water. Oscar Lake contains at least $9.5 \times 10^7 \text{ m}^3$ of water based on limited bathymetry data collected along the margin of the subaerial lake that existed in 2006. The subaerial portion of the lake has expanded rapidly since then, and the lake likely extends a substantial distance underneath the glacier based on measurements and observations at many other glacier-dammed lakes. For example, Anderson et al. (2003) noted that ~20% of the total lake volume at Hidden Creek Lake was contained beneath the ice dam. If Oscar Lake drained to the terminus, Abyss Lake could drain with it. The draining of Oscar Lake would increase the hydraulic head of Abyss Lake by at least 160 m (Fig. 5), thereby increasing the chance of an Abyss jökulhlaup. The combined volume of the two lakes would be at least $3.2 \times 10^8 \text{ m}^3$, but the actual value would likely be much higher considering our conservative lake volume calculations and the volume of water that we are unable to account for underneath the floating ice shelves. A jökulhlaup of the size envisioned here might mechanically erode ice from the terminus by large-scale tunnel collapse, hydraulic jacking, ice-cliff collapse, and other processes.

Russell et al. (2006) also noted that jökulhlaups can incise and extend outwash plains. Stream power and therefore erosion potential are greatest where the jökulhlaup exits the glacier. After a large jökulhlaup, subsequent will be more channelized, further focusing stream power and potentially causing more extensive erosion (Russell et al., 2006). The amount of erosion or deposition at any one location is controlled by slope, discharge, and sediment availability. On the Brady Glacier outwash plain, slope is known and discharge can be estimated, but subglacial sediment availability and potential jökulhlaup routing are unknown. Therefore, we cannot predict the location or magnitude of erosion or deposition at and away from the terminus. Nevertheless, a combined jökulhlaup from Abyss and Oscar lakes could incise the stabilizing outwash plain adjacent to the terminus and cause the glacier to lose contact with it. Repeated events could trigger a return to a tidewater regime.

5.4. Space as a proxy for time

Kastens and Ishikawa (2006, p. 72) stated that '...it is fairly common in thinking about the Earth to find that variation or progression through space is closely connected with variation or progression through time.' As a result we often think about distance in space instead of duration of geologic time. An example of substituting space for time at Brady Glacier comes from using the evolution of South Trick Lake, the lake nearest the terminus and lowest in elevation, to illustrate how lakes higher on Brady Glacier might respond if the glacier continues to downwaste or begins to retreat. We have described how South Trick Lake was dammed by the advancing glacier, released jökulhlaups for decades, then eventually was no longer dammed by the glacier as it downwasted and retreated. Clague and Evans (1994) identified argued that many glacier-dammed lakes go through a similar cycle of jökulhlaup activity as their glacier dams weaken because of downwasting and retreat. A critical threshold is reached when the glacier can no longer impound the lake and a cycle of jökulhlaups begins. With continued downwasting or retreat, the frequency of jökulhlaups

may increase, but the magnitude decreases until eventually the water establishes a permanent outlet and jökulhlaups cease. Using knowledge of the jökulhlaup cycle learned from previous behaviour of Brady and similar glacier systems, we can predict how lakes more distant from the terminus and higher in elevation will evolve through time.

The clearest example of applying the concept of space as a proxy for time in understanding the evolution of Brady Glacier's lakes is the four subglacial lakes. Based on the results of this study and the conclusions reached by Capps et al. (2010), these lakes will become increasingly subaerial if Brady Glacier continues to downwaste and retreat, especially as the calving fronts increase in width and depth, thereby creating a positive feedback cycle for more ice loss. Oscar Lake recently began a rapid subaerial expansion. We expect this expansion to continue until the calving margin retreats to where the lobe of ice flowing into the basin narrows and lateral shear stress provides sufficient drag to once again stabilize the calving margin. Depending on where this stable location is, the retreat could destabilize ice that dams the lake and trigger the first jökulhlaup of record. Saddle and Hinge lakes will likely begin to release jökulhlaups several years after, with Divide Lake beginning last because it is the farthest from the terminus and highest in elevation. The four subglacial lakes will likely parallel Abyss Lake's evolution from subglacial and relatively stable to subaerial with catastrophic outbursts. Geertsema and Clague (2005) documented an example of this type of evolution with Lake No Lake, dammed by Tulsequah Glacier in north-west British Columbia.

5.5. Evolution of analogous glacier/lake systems

5.5.1. Past

There are analogous glacier and lake systems that have evolved in much the same manner that we predict for Brady Glacier. An excellent example is the evolution of Excelsior Glacier and Excelsior Lake in the Kenai Mountains of southern Alaska. In 1913, Excelsior Glacier terminated on an outwash plain about 1 km from Johnstone Bay. In 1941 Excelsior Lake was in the initial stages of development 8 km north-northeast NNE of its 1913 terminus (Fig. 10A; Stone, 1963). The debris-covered ice visible on a 1941 airphoto is likely a suture zone between west-flowing ice from tributary glaciers to the east and east-flowing ice from a distributary of Excelsior Glacier. Also visible in this photo, as indicated by the arrows, are two areas of subaerial lake exposure. By 1951, the terminus of the glacier had retreated as much as 4.3 km into a terminal lake, the area of Excelsior Lake itself had expanded dramatically, and Excelsior Lake had drained (Fig. 10B). Excelsior Lake grew to fill most of its potential tributary basin by the 1960s (Fig. 10C; Marcus, 1968) and is now an embayment in the rapidly enlarging terminal lake (Fig. 10D). We do not know if jökulhlaups from the lake contributed to the breakup of the terminus of the glacier, but the calving dynamics at Excelsior Lake certainly contributed to enhanced breakup of the glacier evident in Fig. 10D.

The geometry of the Excelsior Lake basin is similar to that of the Abyss and Hinge lake basins. In particular, the state of Excelsior Lake in 1941 is similar to the present state of Hinge Lake, which also has small subaerial lakes like those shown in Fig. 10A. Abyss and Hinge lakes and Brady Glacier may go through an evolution similar to that of Excelsior Lake and Excelsior Glacier.

5.5.2. Future

There are analogous glacier and lake systems that may experience an evolution comparable to that at Excelsior Glacier and to that we predict for Brady Glacier. An example is Baird Glacier and a series of lakes that it dams near Petersburg, Alaska (Fig. 11). Baird Glacier currently terminates against a 2-km-long outwash plain about 10 m above Thomas Bay. The glacier downwasted substantially between 1948 and 2000 (Larsen et al., 2007). It presently impounds large volumes of water in the Witches Cauldron, a tributary in which there has been a 9.5-km reversal of ice flow. We infer that jökulhlaups have occurred from a lake at

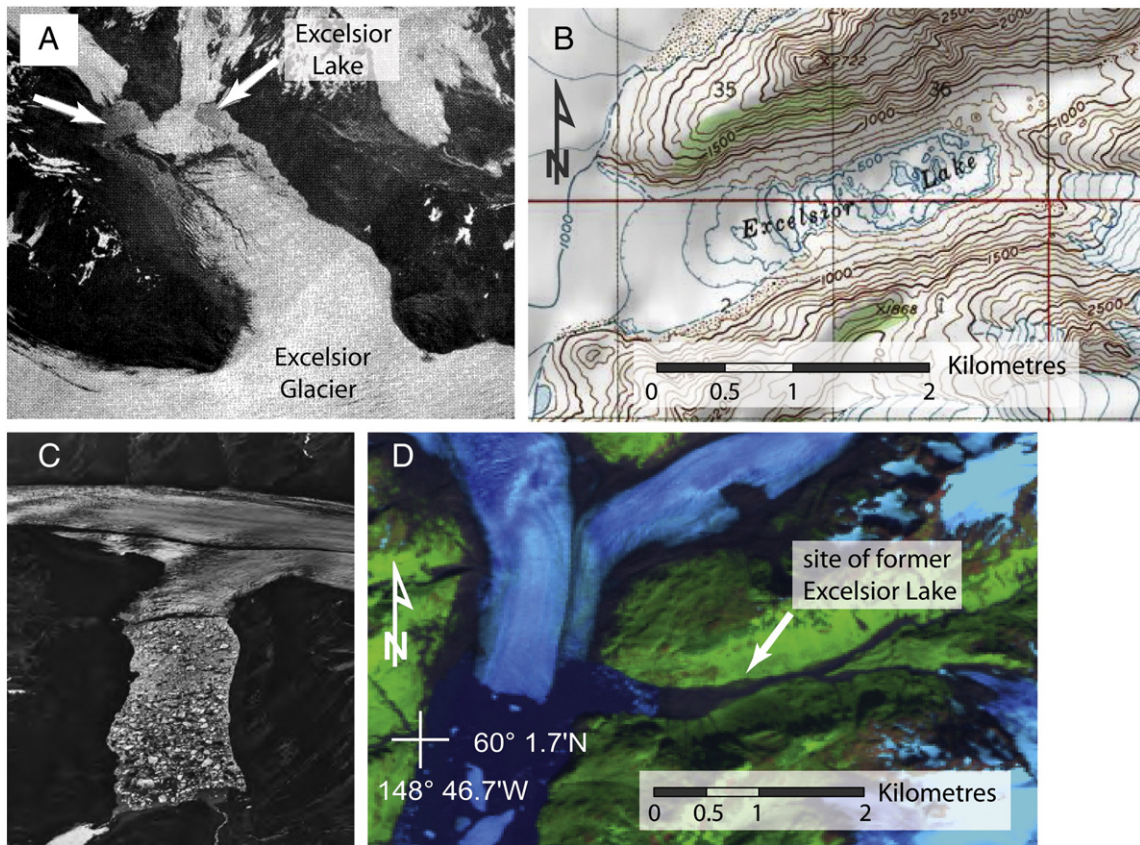


Fig. 10. Evolution of Excelsior Glacier and Excelsior Lake through time. (A) 15 August 1941 oblique airphoto of Excelsior Glacier, view east. Arrows indicate two areas of subaerial lake water (from Stone, 1963). (B) 1951 U.S. Geological Survey 1:63,360 topographic map of Excelsior Lake, contour interval 100 ft (ca. 30 m). (C) 3 September 1966, oblique airphotos of Excelsior Lake, view west (after Molnia, 2008). (D) 30-m resolution, false-colour Landsat 5 image (bands 7/4/2) acquired on 3 August 2009.

the head of this tributary based on observations of stranded icebergs in previous Landsat imagery (Fig. 11). If Baird Glacier continues to downwaste, glacier-dammed lakes in the Witches Cauldron and other tributaries will grow in size and number and the terminus may retreat

off the stabilizing outwash plain. Abandonment of the outwash plain could trigger a catastrophic retreat because Baird Glacier, like Brady Glacier, is probably grounded well below sea level.

There are numerous other examples of glacier-dammed lakes and their associated jökulhlaups that are likely to play a key role in the evolution of glaciers. Examples are the Dead Branch of Norris Glacier near Juneau, which has a conspicuous crevasse along its centre line similar to that at Hinge Lake, Tulsequah Glacier near Juneau, a series of glaciers that dam lakes in the Desolation Valley north of Lituya Bay, and Battle Glacier near Alsek River.

6. Conclusion

Despite small advances and retreats, the main terminus of Brady Glacier has changed little since 1880. However, it has downwasted substantially, more than the regional average of 2–3 m/y, between 1948 and 2000. The most dramatic retreat (2 km) and downwasting (~125 m) have occurred adjacent to glacier-dammed lakes. Retreat and downwasting are primarily the result of glacier dynamics associated with 10 large glacier-dammed lakes. Between 1948 and 2010, the combined calving width of the glacier-dammed lakes increased from 11.5 to 18.3 km. Bathymetry surveys revealed that some lakes contain at least $3.45 \times 10^8 \text{ m}^3$ of water, and jökulhlaups from one or more lakes could have a significant influence on the terminus of the glacier. Brady Glacier is a former tidewater glacier with many glacier-dammed lakes that are contributing to mass loss. Based on observed conditions and predicted climate trends, Brady Glacier may return to a tidewater regime and enter into a phase of catastrophic retreat. The situation at Brady Glacier is not unique, and the lessons learned here can be applied



Fig. 11. 30-m resolution, false-colour Landsat 5 image (bands 7/4/2) of Baird Glacier acquired on 19 September 2010. Note substantial flow reversals (red arrows), source of past jökulhlaups (red asterisk), outwash plain, and tidewater near southwest edge of image.

elsewhere to identify future glacier-dammed lakes, jökulhlaups, and glacier instability.

Acknowledgments

This research was funded through a Canon National Parks Science Scholarship to Capps and a Natural Sciences and Engineering Research Council of Canada Discovery Grant to Clague. We acknowledge Dr. Chris Larsen for generously sharing data; Mike Loverink, owner and pilot of Air Excursions, for his willingness to land a float-plane in iceberg- and snag-infested waters; Dan Shugar for three seasons of assistance with challenging fieldwork; Glacier Bay National Park for maps, aerial photographs, and accommodation; the staff of the SFU Department of Earth Sciences for office assistance; three anonymous reviewers who took the time to greatly improve the manuscript; and Dr. Richard Marston, the editor, who shepherded this paper through the publication process and provided final edits.

Appendix A. Supplementary data

Supplementary data associated with this article can be found in the online version, at <http://dx.doi.org/10.1016/j.geomorph.2013.12.018>. These data include Google map of the most important areas described in this article.

References

- Aðalgeirsdóttir, G., Echelmeyer, K.A., Harrison, W.D., 1998. Elevation and volume changes on the Harding Icefield, Alaska. *J. Glaciol.* 44 (148), 570–582.
- Anderson, S.P., Walder, J.S., Anderson, R.S., Kraal, E.R., Cunico, M., Fountain, A.G., Trabant, D.C., 2003. Integrated hydrologic and hydrochemical observations of Hidden Creek Lake jökulhlaups, Kennicott Glacier, Alaska. *J. Geophys. Res.* 108 (F1), 1–19.
- Anderson, R.S., Walder, J.S., Anderson, S.P., Trabant, D.C., Fountain, A.G., 2005. The dynamic response of Kennicott Glacier, Alaska, USA, to the Hidden Creek Lake outburst flood. *Ann. Glaciol.* 40 (1), 237–242.
- Arendt, A.A., Echelmeyer, K.A., Harrison, W.D., Lingle, C.S., Valentine, V.B., 2002. Rapid wastage of Alaska glaciers and their contribution to rising sea level. *Science* 297 (5580), 382–386.
- Barclay, D.J., Wiles, G.C., Calkin, P.E., 2009. Holocene glacier fluctuations in Alaska. *Q. Sci. Rev.* 28 (21–22), 2034–2048.
- Barnes, D.F., Watts, R.D., 1977. Geophysical surveys in Glacier Bay National Monument. *U.S. Geol. Surv. Circ.* 751-B.
- Bartholomaeus, T.C., Anderson, R.S., Anderson, S.P., 2011. Growth and collapse of the distributed subglacial hydrologic system of Kennicott Glacier, Alaska, USA, and its effects on basal motion. *J. Glaciol.* 57 (206), 985–1002.
- Bengtson, K.B., 1962. Recent history of the Brady Glacier, Glacier Bay National Monument, Alaska, U.S.A. *Int. Assoc. Sci. Hydrol. Int. Union Geodesy Geophys. Symp. Obergurgl* 58, 78–87.
- Capps, D.M., Rabus, B., Clague, J.J., Shugar, D.H., 2010. Identification and characterization of alpine subglacial lakes using interferometric synthetic aperture radar (InSAR): Brady Glacier, Alaska, USA. *J. Glaciol.* 56 (199), 861–870.
- Capps, D.M., Wiles, G.C., Clague, J.J., Luckman, B.H., 2011. Tree-ring dating of the nineteenth-century advance of Brady Glacier and the evolution of two ice-marginal lakes, Alaska. *The Holocene* 21 (4), 641–649.
- Clague, J.J., Evans, S.G., 1994. Formation and failure of natural dams in the Canadian Cordillera. *Geol. Surv. Can. Bull.* 464.
- Derksen, S.J., 1976. Glacial geology of the Brady Glacier region, Alaska. *Inst. Polar Stud. Rep.* 60.
- Geertsema, M., Clague, J.J., 2005. Jökulhlaups at Tulsequah Glacier, northwestern British Columbia, Canada. *Holocene* 15 (2), 310–316.
- Geirsdóttir, Á., Miller, G.H., Wattrus, N.J., Björnsson, H., Thors, K., 2008. Stabilization of glaciers terminating in closed water bodies: evidence and broader implications. *Geophys. Res. Lett.* 35, L17502.
- Grover, J.S., 2003. An investigation of glacier outburst floods from Abyss Lake, Glacier Bay National Park, Alaska. *Nat. Res. Tech. Report 312*, Nat. Park Serv., Nat. Res. Water Res. Div. Ft. Collins, CO.
- Hughes, M.L., McDowell, P.F., Marcus, W.A., 2006. Accuracy assessment of georectified aerial photographs: implications for measuring lateral channel movement in a GIS. *Geomorphology* 74 (1–4), 1–16.
- International Boundary Commission, 1923. Alaska Boundary Tribunal Map Series (1907): #10 from Cape Muzon to Mount St. Elias. *Intern. Boundary Comm. Ottawa, ON*, scale 1:250,000.
- Kastens, K.A., Ishikawa, T., 2006. Spatial thinking in the geosciences and cognitive sciences: a cross-disciplinary look at the intersection of the two fields. In: Manduca, C.A., Mogk, D.W. (Eds.), *Earth and Mind: How Geologists Think and Learn about the Earth*. *Geol. Soc. Am. Spec. Paper*, 413, pp. 53–76.
- Larsen, C.F., Motyka, R.J., Arendt, A.A., Echelmeyer, K.A., Geissler, P.E., 2007. Glacier changes in southeast Alaska and northwest British Columbia and contribution to sea level rise. *J. Geophys. Res.* 112 (F01007), 1–11.
- Magnússon, E., Björnsson, H., Rott, H., Pálsson, F., 2010. Reduced glacier sliding caused by persistent drainage from a subglacial lake. *Cryosphere* 4 (2), 13–20.
- Marcus, M.G., 1960. Periodic drainage of glacier-dammed Tulsequah Lake, British Columbia. *Geogr. Rev.* 50 (1), 89–106.
- Marcus, M.G., 1968. Effects on glacier-dammed lakes in the Chugach and Kenai Mountains. *The Great Alaska Earthquake: Hydrology. Part A. Nat. Acad. Sci. Washington, DC*, pp. 329–347.
- Mason, K., Gunn, J.P., Todd, H.J., 1930. The Shyok flood, 1929. *Himal. J.* 2, 35–47.
- Mayer, C., Lambrecht, A., Hagg, W., Helm, A., Scharrer, K., 2008. Post-drainage ice dam response at Lake Merzbacher, Inylchek Glacier, Kyrgyzstan. *Geogr. Ann.* 90A (1), 87–96.
- Meier, M.F., Post, A., 1987. Fast tidewater glaciers. *J. Geophys. Res.* 92 (B9), 9051–9058.
- Molnia, B.F., 2008. *Satellite Image Atlas of Glaciers of the World; Glaciers of North America; Glaciers of Alaska*. *U.S. Geol. Surv. Prof. Pap.* 1386-K.
- Muir, J., 1915. *Travels in Alaska*. Houghton Mifflin Co., New York.
- Pelto, M., Capps, D., Clague, J.J., Pelto, B., 2013. Rising ELA and expanding proglacial lakes indicate impending rapid retreat of Brady Glacier, Alaska. *Hydrol. Process.* 27 (21), 3075–3082.
- Post, A., Mayo, L.R., 1971. Glacier dammed lakes and outburst floods in Alaska. *U.S. Geol. Surv. Hydrol. Invest. Atlas* HA-455.
- Russell, A.J., Roberts, M.J., Fay, H., Marren, P.M., Cassidy, N.J., Tweed, F.S., Harris, T., 2006. Icelandic jökulhlaup impacts: implications for ice-sheet hydrology, sediment transfer and geomorphology. *Geomorphology* 75 (1–2), 33–64.
- Stone, K.H., 1963. Alaskan ice-dammed lakes. *Ann. Assoc. Am. Geogr.* 53 (3), 332–349.
- Sugiyama, S., Bauder, A., Weiss, P., Funk, M., 2007. Reversal of ice motion during the outburst of a glacier-dammed lake on Gornerglletscher, Switzerland. *J. Glaciol.* 1 (181), 75–84.
- Tweed, F.S., Russell, A.J., 1999. Controls on the formation and sudden drainage of glacier-impounded lakes: implications for jökulhlaup characteristics. *Prog. Phys. Geogr.* 23 (1), 79–110.
- van der Veen, C.J., 2002. Calving glaciers. *Prog. Phys. Geogr.* 26 (1), 96–122.
- Vancouver, G., 1798. *A Voyage of Discovery to the North Pacific Ocean, and Round the World: In which the Coast of North-west America has been Carefully Examined and Accurately Surveyed: Undertaken by His Majesty's Command, Principally with a View to Ascertain the Existence of Any Navigable Communication Between the North Pacific and North Atlantic Oceans, and Performed in the Years 1790, 1791, 1792, 1793, 1794, and 1795, in the Discovery Sloop of War, and Armed Tender Chatham, Under the Command of Captain George Vancouver, Volume III. Pall-Mall, London* (Printed for G.G. and J. Robinson, Paternoster Row and J. Edwards).
- Viens, R.J., 1995. Dynamics and mass balance of temperate tidewater calving glaciers of southern Alaska. M.S. dissertation, University of Washington, Seattle, WA (149 pp.).
- Walder, J.S., Trabant, D.C., Cunico, M., Fountain, A.G., Anderson, S.P., Anderson, R.S., Malm, A., 2006. Local response of a glacier to annual filling and drainage of an ice-marginal lake. *J. Glaciol.* 52 (178), 440–445.